

## Enhancing detection sensitivity of piezoelectric plate sensor by increasing transverse electromechanical coupling constant

Wei Wu, Wan Y. Shih, and Wei-Heng Shih

Citation: *J. Appl. Phys.* **114**, 064505 (2013); doi: 10.1063/1.4817762

View online: <http://dx.doi.org/10.1063/1.4817762>

View Table of Contents: <http://jap.aip.org/resource/1/JAPIAU/v114/i6>

Published by the AIP Publishing LLC.

---

### Additional information on J. Appl. Phys.

Journal Homepage: <http://jap.aip.org/>

Journal Information: [http://jap.aip.org/about/about\\_the\\_journal](http://jap.aip.org/about/about_the_journal)

Top downloads: [http://jap.aip.org/features/most\\_downloaded](http://jap.aip.org/features/most_downloaded)

Information for Authors: <http://jap.aip.org/authors>

## ADVERTISEMENT



**AIP Advances**

Now Indexed in Thomson Reuters Databases

Explore AIP's open access journal:

- Rapid publication
- Article-level metrics
- Post-publication rating and commenting

## Enhancing detection sensitivity of piezoelectric plate sensor by increasing transverse electromechanical coupling constant

Wei Wu,<sup>1</sup> Wan Y. Shih,<sup>2</sup> and Wei-Heng Shih<sup>1</sup>

<sup>1</sup>Department of Materials Science and Engineering, Drexel University Philadelphia, Pennsylvania 19010, USA

<sup>2</sup>School of Biomedical Engineering, Science, and Health Systems, Drexel University, Philadelphia, Pennsylvania 19010, USA

(Received 9 June 2013; accepted 23 July 2013; published online 12 August 2013)

In this study, we examined how the materials' properties of a lead magnesium niobate-lead titanate solid solution,  $[\text{Pb}(\text{Mg}_{1/3}\text{Nb}_{2/3})\text{O}_3]_{0.63}[\text{PbTiO}_3]_{0.37}$  (PMN-PT) piezoelectric plate sensor (PEPS) affected the enhancement of the relative detection resonance frequency shift,  $-\Delta f/f$  of the sensor, where  $f$  and  $\Delta f$  were the resonance frequency and resonance frequency shift of the sensor, respectively. Specifically, the electromechanical coupling constant,  $-k_{31}$ , of the PMN-PT PEPS was varied by changing the grain size of the piezoelectric layer as well as by applying a bias direct current electric field. Detection of streptavidin at the same concentration was carried out with biotin covalently immobilized on the surface of PEPS. It is shown that the  $-\Delta f/f$  of the same streptavidin detection was increased by more than 2-fold when the  $-k_{31}$  increased from 0.285 to 0.391. © 2013 AIP Publishing LLC. [<http://dx.doi.org/10.1063/1.4817762>]

### I. INTRODUCTION

Current protein detection relies on optical, label-based methods such as enzyme linked immuno-sorbent assay (ELISA), which is tedious and time consuming as it requires multiple steps of binding and washing and does not lend itself for multiplexing. In the past two decades, label-free alternatives have been studied by many authors. Some of the examples include quartz crystal microbalance (QCM),<sup>1–3</sup> surface acoustic wave (SAW) devices,<sup>4,5</sup> surface plasmon resonance (SPR),<sup>6,7</sup> silicon microcantilevers,<sup>8–11</sup> electrochemical sensors,<sup>12–14</sup> nanotube and nanowire biosensors.<sup>15–17</sup> Although these label-free methods can be rapid and simpler, they generally lack the sensitivity of ELISA. As a result, many have investigated ways to improve the detection sensitivities of these label-free sensors. These efforts invariably focused on either improving the orientation of the receptors on the sensor surface,<sup>18,19</sup> or amplifying the detection signal through incorporating secondary antibody-linked enzymes in electrochemical detections,<sup>20</sup> or through geometry optimization and size reduction such as in silicon micro-/nano-cantilevers,<sup>21</sup> or by incorporating a secondary antibody or a secondary antibody-linked nanoparticles.<sup>22,23</sup> So far, no studies have focused on improving a sensor's sensing performance through the sensor's materials property improvement.

Piezoelectric microcantilever sensors (PEMSs)<sup>24–27</sup> are a relatively new type of sensor with high sensitivity, consisting of a highly piezoelectric layer made of lead zirconate-lead titanate (PZT)<sup>27</sup> or lead magnesium niobate-lead titanate (PMN-PT)<sup>24–26</sup> bonded to a nonpiezoelectric layer. More recently, the piezoelectric plate sensor (PEPS)<sup>28</sup> was developed and used solely as a highly piezoelectric plate without the nonpiezoelectric layer. With receptors immobilized on a PEMS/PEPS surface, binding of target analytes can shift the resonance frequency of the PEMS/PEPS. Detection of target analytes is achieved by electrically monitoring the resonance frequency shift of the PEMS/PEPS, offering the potential

of real-time, *in situ* detection of chemical and biological analytes. PEMS and PEPS have shown high detection sensitivity in a variety of analyte detection such as human epidermal growth factor receptor 2 (Her2),<sup>24,25</sup> white spot syndrome virus,<sup>26</sup> Bacillus anthracis,<sup>27</sup> and DNA detection<sup>28</sup> and the high detection sensitivity was due to enhancement of the detection resonance frequency that could be as high as three orders of magnitude higher than could be accounted by mass change alone.<sup>29–32</sup> In this study, we intend to examine how the materials properties of the piezoelectric layer affect the enhancement of the resonance frequency shift of the sensor.

The enhancement of the detection resonance frequency shift of PEMS and PEPS has previously been shown to be related to the Young's modulus change due to the polarization orientation switching in the piezoelectric layer as a result of the surface stress generated by the bound target analytes on the sensor surface.<sup>30–32</sup> It is known that polarization switching capability in a soft piezoelectric such as PMN-PT can be controlled by the grain size of the piezoelectric as grain boundaries have been shown to inhibit polarization domain switching.<sup>33,34</sup> For example, Randall *et al.*<sup>35</sup> showed that the piezoelectric coefficients,  $d_{33}$  and  $-d_{31}$ , and electromechanical coupling constants,  $-k_{31}$  and  $-k_p$ , of PZT ceramics increased with an increasing grain size due to the extrinsic contributions of domain switching. Similar grain size effects on piezoelectric properties were also found in PMN-PT,<sup>36</sup> lead nickel niobate-lead zirconate titanate (PNN-PZT),<sup>37</sup> and in lead-free piezoelectrics such as sodium potassium niobate.<sup>38</sup> Piezoelectric thin films with a larger grain size were also shown to exhibit better  $d_{33}$  and  $-d_{31}$  coefficients at the same thickness.<sup>39–41</sup> These examples indicate the possibility of changing the grain size of the piezoelectric layer as a way of controlling the polarization switching capability and hence the enhancement of detection sensitivity of a PEPS. Furthermore, in a separate study, Zhu *et al.* showed that by applying a negative direct current (DC) bias electric field, the

detection resonance frequency shift of a PMN-PT/Cu PEMS was enhanced by more than two times.<sup>31</sup> This experiment indicated that applying a DC bias electric field could also be a way of controlling the polarization switching capability to affect the detection sensitivity of a PMN-PT PEPS.

Since it is well-accepted that the electromechanical coupling constant is closely related to the polarization domain switching capability of a soft piezoelectric, one can use electromechanical coupling constant as a gauge of domain switching capability to correlate with a PEMS/PEPS detection sensitivity enhancement.

The purpose of this study is to implement different domain switching capability in a PMN-PT PEPS and correlate the  $-k_{31}$  coupling coefficient of the PMN-PT layer to the relative detection resonance frequency change,  $\Delta f/f$ , where  $f$  and  $\Delta f$  stand for the resonance frequency and the detection resonance frequency change of the PEPS. For this study, we will use the same procedure to immobilize biotin on the surface of all PEPS and use the biotin modified PEPS to detect streptavidin under the same condition. Although changing the  $-k_{31}$  constant will also enhance the detection frequency change of a PEMS, the reason we focus our study on PEPS is that the PEPS is mainly consisted of a piezoelectric layer, whereas a PEMS has an additional nonpiezoelectric layer which may complicate the interpretation. To implement changes in the  $-k_{31}$  of PEPSs, we will (1) fabricate PEPSs from PMN-PT layers of the same thickness but with different grain sizes and (2) apply various DC bias electric fields to a PEPS during detection.

## II. EXPERIMENTAL

### A. Fabrication of PMN-PT thin sheets of different $-k_{31}$

To fabricate PMN-PT freestanding sheets, thin PMN-PT tapes were cast using a PMN-PT precursor powder synthesized using a double colloidal-coating method.<sup>42</sup> To control the  $-k_{31}$  of a PMN-PT layer, we sintered the PMN-PT green tapes under different PbO vapor pressure because PbO will become a liquid phase during the sintering and can be used as a sintering aid to vary grain size. To control the grain size, we used a double-crucible approach during sintering. First, we placed a 10 mm  $\times$  10 mm PMN-PT green tapes (12  $\mu$ m thick) on a flat alumina plate and placed 0.2 g of a PbO powder (99.9%, Alfa Aesar) in a small partially covered alumina crucible. We then placed both the sample containing alumina plate and the PbO containing small alumina crucible inside a large covered alumina crucible for sintering. The temperature was increased at 1  $^{\circ}$ C/min below 400  $^{\circ}$ C and 10  $^{\circ}$ C/min above 400  $^{\circ}$ C and held at 1150  $^{\circ}$ C for 2 h. The small crucible helped control the PbO partial pressure inside the large crucible, while the covered large crucible helped minimize loss of PbO to the furnace. The grain size of the PMN-PT thin sheet was controlled by the size of the opening of the small crucible.

### B. PEPS fabrication

In the study, nine PEPSs were made from 8  $\mu$ m-thick PMN-PT thin sheets with various grain sizes. Each PEPS was about 1.0 mm in length and 0.7 mm in width with one

end fixed on a substrate. The photograph of a typical PEPS is shown in Fig. 1(a). Briefly, 150 nm thick gold electrodes were deposited on both sides of a PMN-PT sheet with a 50 nm chromium bonding layer by thermal evaporation (Thermionics VE 90). The gold-coated PMN-PT thin sheets were then cut into 0.6–1.0 mm  $\times$  1.8–2.3 mm rectangular strips using a wire saw (Princeton Scientific Precision, Princeton, NJ). Gold wires of 10  $\mu$ m diameter were attached to each side of the strips as leads and glue to the substrate using a non-conducting glue for ease of handling. The PEPSs were poled with an electric field of 15 KV/cm at 80  $^{\circ}$ C for 30 min on a hotplate. After poling, PEPS's dielectric constant was measured using an impedance analyzer (4294A, Agilent).

### C. Electrical insulation

For electrical insulation, we followed an optimized wet-chemical deposition method developed by Soylyu *et al.*<sup>43</sup> First, a PEPS was cleaned in a 1-in-40 diluted piranha solution (piranha solution is a 3:1 mixture of sulfuric acid and 30% hydrogen peroxide) for 10 min followed by de-ionized (DI) water and ethanol rinsing. It was then soaked in a 0.1 mM mercaptopropyltrimethoxysilane (MPS) (Sigma) solution in ethanol (Fisher) with 0.1% DI water for 30 min followed by soaking in a 0.1% MPS solution in ethanol with 0.5% DI water at pH 9 for 48 h where the MPS solution was replaced with a fresh one every 12 h. For each MPS solution replacement, the PEPS was first rinsed with DI water and followed by ethanol before immersing in a fresh MPS solution. Finally, the PEPS was rinsed with DI water and ethanol before further surface modification for detection.

### D. Determination of $-k_{31}$

A PEPS typically exhibits strong resonance peaks associated with the first length extension mode (LEM) (Fig. 1(b)) and width extension mode (WEM) vibrations (Fig. 1(c)). The resonance spectrum and the dielectric constant of a PEPS were measured using an impedance analyzer (Agilent, 4294A). As an example, the in-air and in-phosphate buffer saline (PBS) resonance spectra of a MPS-coated PEPS that had a  $-k_{31} = 0.340$  are shown in Fig. 2(a).

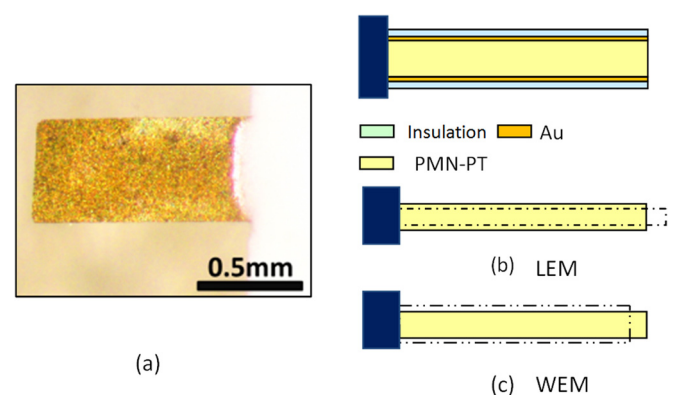


FIG. 1. (a) An optical micrograph of a PEPS viewed from the top surface, and (b) and (c) are schematics of the LEM and the WEM vibrations.

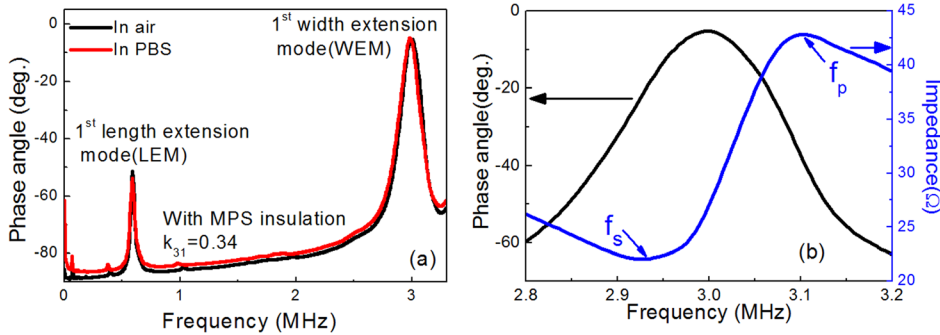


FIG. 2. (a) The phase-angle-versus-frequency resonance spectra of a  $8.0\ \mu\text{m}$  PMN-PT PEPS coated with MPS insulation in-air and in-PBS and (b) the electrical impedance (blue) and phase angle (black) versus frequency of the PEPS in (a) around the WEM peak from which  $k_{31}$  was deduced, where  $f_s$  and  $f_p$  are the series and parallel resonance frequencies approximated as the minimum and maximum of the impedance, respectively.

For a piezoelectric plate with an electric field applied in the thickness direction such as in a PEPS, the  $-k_{31}$  could be deduced from the WEM peak using the following equation:<sup>44</sup>

$$\frac{k_{31}^2}{1 - k_{31}^2} = \frac{\pi f_p}{2 f_s} \tan\left(\frac{\pi f_p - f_s}{2 f_s}\right), \quad (1)$$

where  $f_s$  and  $f_p$  were the series and parallel resonant frequencies approximated as the minimum and maximum of the electrical impedance versus frequency plot around the WEM resonance peak as illustrated in Fig. 2(b).

### E. Model streptavidin detection

Biotin-streptavidin-biotin is a well-established receptor immobilization scheme.<sup>45</sup> For present study, we covalently immobilized biotin on the sensor surface and used biotin-coated PEPS to detect streptavidin as the model detection. To covalently immobilize biotin on a PEPS surface, a MPS-coated PEPS is immersed in  $100\ \mu\text{l}$  of  $2\ \mu\text{M}$  maleimide-polyethylene glycol (PEG)-biotin (Thermo scientific, IL) for 30 min for the maleimide of the maleimide-PEG-biotin reacted with the thiol group of the MPS surface as schematically shown in Fig. 3(a) to covalently immobilize biotin

on the PEPS surface. The PEPS was then rinsed in PBS for three times followed by soaking in PBS for 20 min to monitor the resonance peak stability to ensure that the electrical insulation was adequate and the PEPS was stable in PBS. Once we made sure that the PEPS was stable, the PEPS was then placed in a  $0.1\ \text{mg/ml}$  streptavidin solution in PBS for 30 min at room temperature to allow streptavidin to bind to the immobilized biotin on the PEPS surface as schematically shown in Fig. 3(b). It was this streptavidin-biotin binding period in which the LEM resonance frequency of the PEPS was measured for the model streptavidin detection.

## III. RESULTS AND DISCUSSIONS

### A. $-k_{31}$ as a function of grain size

By controlling PbO vapor pressure during sintering, PMN-PT thin sheets of different grain sizes ranging from  $0.6$  to  $6\ \mu\text{m}$  could be obtained. As examples, Figs. 4(a)–4(h) show the cross-section scanning electron microscopy (SEM) (FEI XL30) micrographs of PMN-PT sheets of different grain sizes. In Fig. 5(a), we plot the  $-k_{31}$  versus  $G$ , where  $G$  is the average grain size of each PEPS as determined from the SEM micrographs. Also plotted is the dielectric constant ( $\epsilon$ ) versus  $G$ . As can be seen,  $\epsilon$  also increased with an

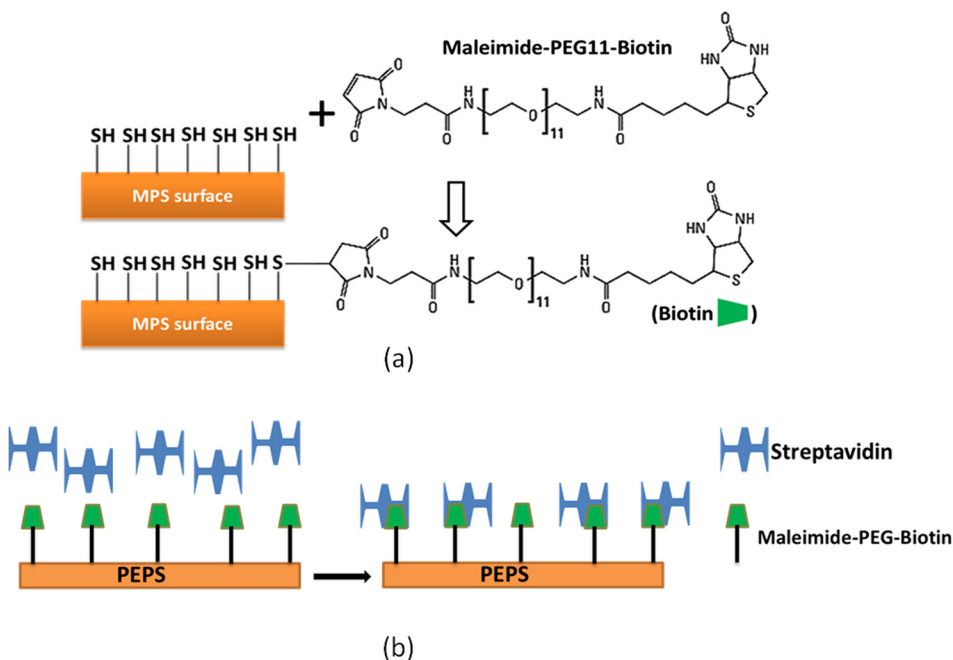


FIG. 3. (a) A schematic of biotin immobilization reaction on a PEPS surface and (b) a schematic of PEPS detection of streptavidin binding to the immobilized biotin.

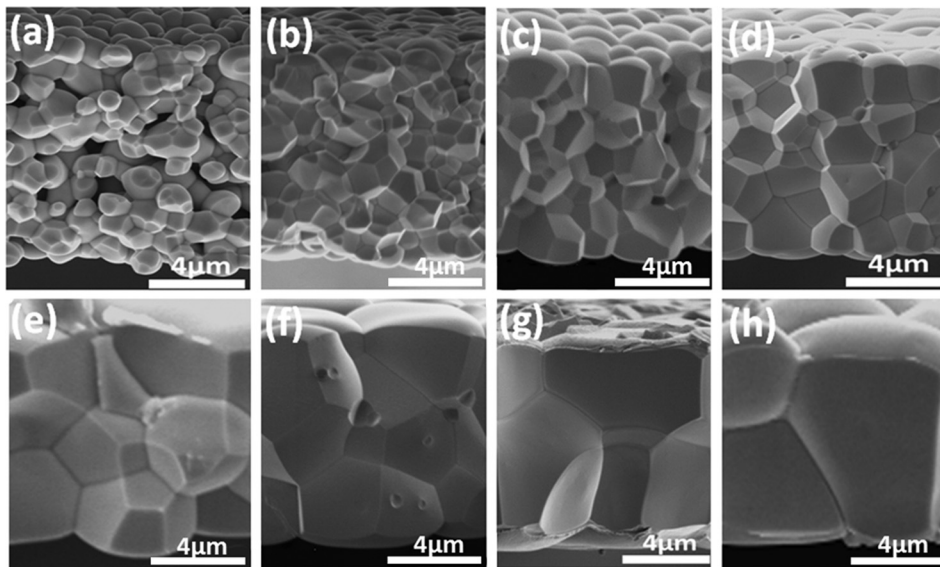


FIG. 4. SEM micrographs of 8  $\mu\text{m}$  thick PMN-PT of different grain sizes,  $G$ , by different sintering conditions: (a)  $G = 0.6 \mu\text{m}$ ; (b)  $G = 1.0 \mu\text{m}$ ; (c)  $G = 1.6 \mu\text{m}$ ; (d)  $G = 2.3 \mu\text{m}$ ; (e)  $G = 2.7 \mu\text{m}$ ; (f)  $G = 3.4 \mu\text{m}$ ; (g)  $G = 4.0 \mu\text{m}$ ; (h)  $G = 6.0 \mu\text{m}$ .

increasing grain size. This result was consistent with the fact that grain boundaries acted as barriers for polarization orientation switching. As the grain size increased, the density of grain boundaries decreased thereby reducing the density of barriers of polarization switching. In fact, as can be seen,  $-k_{31}$  increased with an increasing  $G$  as  $-k_{31} \propto \log(G)$ , similar to the results of Randall *et al.*<sup>35</sup> Also shown in Fig. 5(a) is dielectric constant,  $\epsilon$ , versus  $G$ , which also exhibited a logarithmic behavior with grain size for fully dense PMN-PT polycrystals.

### B. $-\Delta f/f$ as a function of $-k_{31}$ through grain size engineering

Model streptavidin detection using PEPSs with different  $-k_{31}$  (or grain sizes) was carried out as described above. As an example, we showed the  $\Delta f/f$  as a function of detection time of PEPSs with  $-k_{31} = 0.301$  (circles), 0.322 (triangles), and 0.340 (squares), respectively, in Fig. 5(b) in which the first 15–20 min was for PEPS stability monitoring and the streptavidin detection was carried out between  $t = 20$  and 50 min.

The magnitude of the final  $\Delta f/f$  was larger for a PEPS with a larger  $-k_{31}$ . We use the value of  $-\Delta f/f$  (an adjacent average of 5 data points) at  $t = 50$  min as a measure of the sensor performance to correlate with  $-k_{31}$ . The results are shown in Fig. 5(c). It can be seen from Fig. 5(c) that  $-\Delta f/f$  increased with increasing  $-k_{31}$ . Note that not all PEPS have the same length and width, as a result, the resonance shift,  $-\Delta f$ , contained the effect of sensor geometry. To remove the effect due to the geometry of the sensor, we used the relative resonance frequency shift  $-\Delta f/f$  as a measure of sensor performance. That a larger  $-k_{31}$  gave rise to a larger  $-\Delta f/f$  was understandable since the coupling constant  $-k_{31}$  of a soft piezoelectric such as PMN-PT was mostly due to the extrinsic effect of polarization orientation switching at room temperature<sup>46</sup> and the relative detection resonance frequency shift  $-\Delta f/f$  was a result of the piezoelectric layer's Young's modulus change due to the polarization orientation switching induced by the surface stress generated by the binding

of the target molecules to the sensor surface.<sup>30,32</sup> Thus, by increasing the  $-k_{31}$  of a PEPS the relative resonance frequency shift,  $-\Delta f/f$ , of the PEPS for the same detection was enhanced.

### C. $-\Delta f/f$ as a function of $-k_{31}$ via DC bias electric field

The electromechanical coupling constant  $-k_{31}$  could also be increased by applying a DC bias electric field. As an example, we plot  $-k_{31}$  and the dielectric constant ( $\epsilon$ ) versus a DC bias electric field,  $E$  in Fig. 6(a). Both  $-k_{31}$  and  $\epsilon$  increased with an increasing DC bias electric field,  $E$ , regardless whether the electric field was parallel (positive  $E$ ) or opposite (negative  $E$ ) to the poling direction. This was due to the fact in PMN-PT thin sheets, the polarization that was opposite to the applied electric field went through a two-step switching process. The polarization first switched to a lateral direction at an intermediate electric field before it finally switched to the parallel direction to the electric field.<sup>47</sup> In the intermediate electric field range, both  $-k_{31}$  and  $\epsilon$  increased as there were more domains with lateral polarization orientations, which were known to exhibit a larger  $-k_{31}$  and  $\epsilon$ .<sup>48</sup> For the current study, we only explored DC bias electric fields in the range where the polarization was switched to the lateral direction as schematically illustrated in Fig. 6(b). As a result, in this electric field range,  $-k_{31}$  and  $\epsilon$  increased with an increasing magnitude of the DC bias electric field. We carried out the same streptavidin detection using the same sensor but with a different DC bias electric field. The result is shown in Fig. 6(c), where  $-\Delta f/f$  is plotted as a function of  $-k_{31}$ . As can be seen, the  $-\Delta f/f$  also increased with an increasing electric field-enhanced  $-k_{31}$ .

Finally, we combined the results in Figs. 5(c) and 6(c) in Fig. 7, where  $-\Delta f/f$  is plotted versus  $-k_{31}$  regardless whether the  $-k_{31}$  value was obtained by changing the grain size or by applying a DC bias electric field. As shown in Fig. 7, there is a universal correlation between  $-\Delta f/f$  and  $-k_{31}$  regardless how the value of  $-k_{31}$  was obtained. This indicates that the electromechanical coupling constant  $-k_{31}$  was a determining parameter for PEPS detection performance. By changing the PEPS

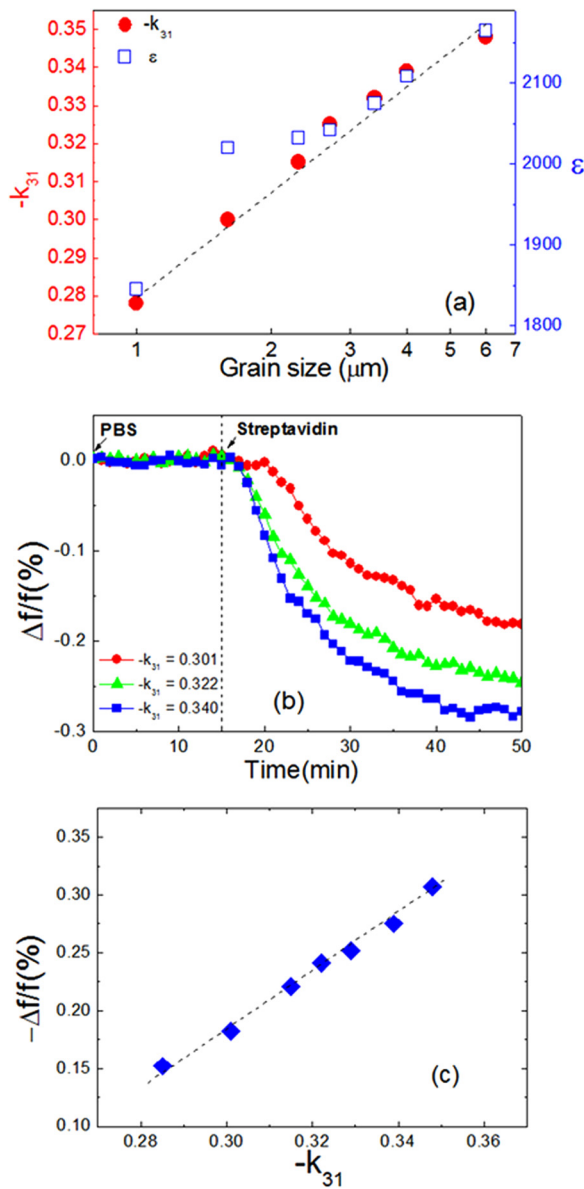


FIG. 5. (a)  $-k_{31}$  and dielectric constant ( $\epsilon$ ) as a function of grain size, (b) examples of  $\Delta f/f$  as a function of detection time for model streptavidin detection using PEPSs with different  $-k_{31}$ , and (c)  $-\Delta f/f$  at time = 50 min as a function of  $-k_{31}$  of the model streptavidin detection for PEPSs with different  $-k_{31}$ .

grain size or applying a DC bias electric field,  $-k_{31}$  could be increased, which enhanced the detection sensitivity ( $-\Delta f/f$ ) of the PEPS. Furthermore, by comparing the results of the same streptavidin detection with a 5-MHz QCM, it was concluded that a PEPS with a  $-k_{31} = 0.32$  had a 1000-fold enhancement on the  $-\Delta f/f$  as compared to that of purely mass detection, resulting in positive detection of DNA with attomolar sensitivity.<sup>28</sup> The present study indicates that by increasing the grain size and by applying a DC bias electric field,  $-k_{31}$  of a PEPS can be increased further to about 0.36-0.40 which had a  $-\Delta f/f$  about 1.5 times that of  $-k_{31} = 0.32$ , implying that the concentration sensitivity of a PEPS can be further improved by such an improved  $-k_{31}$ . How an increased  $-k_{31}$  of a PEPS improves its detection concentration sensitivity will be examined in a future publication.

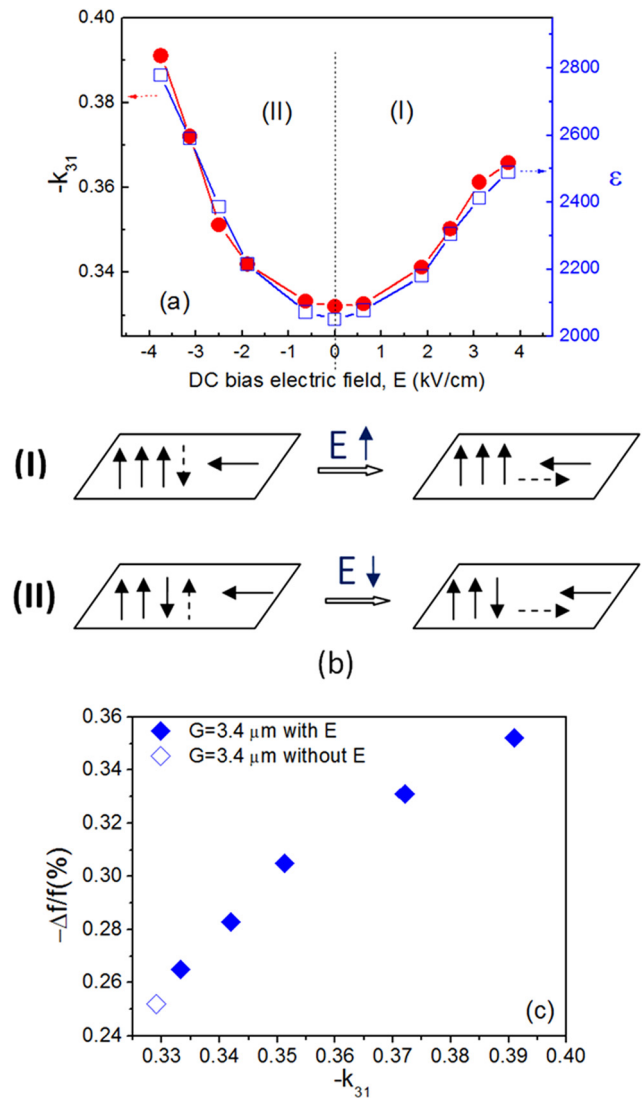


FIG. 6. (a)  $-k_{31}$  (full circles) and dielectric constant ( $\epsilon$ ) (open square) as a function of DC bias electric field,  $E$  of the PEPS with grain size  $G = 3.4 \mu\text{m}$ , (b) schematics illustrating how polarization is switched in a positive (I) and a negative (II) DC bias electric field, and (c) relative frequency shift,  $-\Delta f/f$ , at  $t = 30$  min versus  $-k_{31}$  of the PEPS with  $G = 3.4 \mu\text{m}$  with various DC bias electric fields,  $E$ .

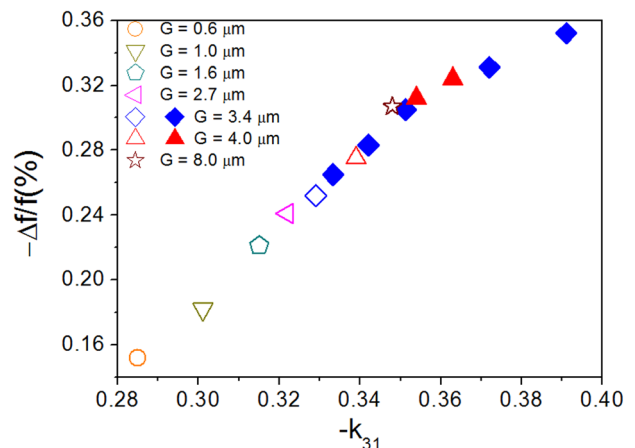


FIG. 7. A summary of relative frequency shift,  $-\Delta f/f$ , as a function of  $-k_{31}$  for PEPS of various grain sizes with (full symbols) and without (open symbols) a DC bias electric field,  $E$ .

#### IV. CONCLUSIONS

In summary, it is shown that the detection relative resonance frequency shift of a PEPS could be enhanced by increasing the electromechanical coupling constant  $-k_{31}$  of the PMN-PT sheet. The  $-k_{31}$  of the PEPS could be increased with an increasing grain size of the PMN-PT thin sheet or by applying a DC bias electric field during detection.

#### ACKNOWLEDGMENTS

This work was supported in part by the Coulter-Drexel Translational Research Partnership grant and the Nanotechnology Institute of Benjamin Franklin Partnership of Southeastern Pennsylvania.

- <sup>1</sup>R. Hart, E. Ergezen, R. Lec, and H. M. Noh, *Biosens. Bioelectron.* **26**, 3391 (2011).
- <sup>2</sup>X. Guo, C.-S. Lin, S.-H. Chen, R. Ye, and V. C. H. Wu, *Biosens. Bioelectron.* **38**, 177 (2012).
- <sup>3</sup>Y. Uludag and I. E. Tothill, *Anal. Chem.* **84**, 5898 (2012).
- <sup>4</sup>F. Di Pietrantonio, D. Cannatà, M. Benetti, E. Verona, A. Varriale, M. Staiano, and S. D'Auria, *Biosens. Bioelectron.* **41**, 328 (2013).
- <sup>5</sup>J.-L. Vivancos, Z. Rácz, M. Cole, and J. W. Gardner, *Sens. Actuators B* **171–172**, 469 (2012).
- <sup>6</sup>K. Pimková, M. Bocková, K. Hegnerová, J. Suttar, J. Čermák, J. Homola, and J. E. Dyr, *Anal. Bioanal. Chem.* **402**, 381 (2012).
- <sup>7</sup>H. Šípová, V. Ševců, M. Kuchař, J. N. Ahmad, P. Mikulecký, R. Osička, P. Malý, and J. Homola, *Sens. Actuators B* **174**, 306 (2012).
- <sup>8</sup>N. Noeth, S. S. Keller, and A. Boisen, *J. Micromech. Microeng.* **21**, 054022 (2011).
- <sup>9</sup>J. Park, S. L. Karsten, S. Nishida, H. Kawakatsu, and H. Fujita, *Lab Chip* **12**, 4115 (2012).
- <sup>10</sup>R. P. Peng, B. Chen, H. F. Ji, L. Z. Wu, and C. H. Tung, *Analyst* **137**, 1220 (2012).
- <sup>11</sup>E. Timurdogan, B. E. Alaca, I. H. Kavakli, and H. Urey, *Biosens. Bioelectron.* **28**, 189 (2011).
- <sup>12</sup>B. Y. Zhao, Q. Wei, C. Xu, H. Li, D. Wu, Y. Cai, K. Mao, Z. Cui, and B. Du, *Sens. Actuators B* **155**, 618 (2011).
- <sup>13</sup>S. Viswanathan, C. Rani, and J.-a. A. Ho, *Talanta* **94**, 315 (2012).
- <sup>14</sup>T. A. Webster and E. D. Goluch, *Lab Chip* **12**, 5195 (2012).
- <sup>15</sup>G.-J. Zhang, M. J. Huang, J. A. J. Ang, Q. Yao, and Y. Ning, *Anal. Chem.* **85**, 4392 (2013).
- <sup>16</sup>R. Yu, C. Pan, and Z. L. Wang, *Energy Environ. Sci.* **6**, 494 (2013).
- <sup>17</sup>P. Sahoo, S. Suresh, S. Dhara, G. Saini, S. Rangarajan, and A. K. Tyagi, *Biosens. Bioelectron.* **44**, 164 (2013).
- <sup>18</sup>A. Singh, D. Arutyunov, M. T. McDermott, C. M. Szymanski, and S. Evoy, *Analyst* **136**, 4780 (2011).
- <sup>19</sup>J.-a. A. Ho, W.-L. Hsu, W.-C. Liao, J.-K. Chiu, M.-L. Chen, H.-C. Chang, and C.-C. Li, *Biosens. Bioelectron.* **26**, 1021 (2010).
- <sup>20</sup>G. Lai, F. Yan, and H. Ju, *Anal. Chem.* **81**, 9730 (2009).
- <sup>21</sup>L. Yang-Choon, A. Z. Kouzani, D. Wei, and A. Kaynak, "Effects of design parameters on sensitivity of microcantilever biosensors," in *2010 IEEE/ICME International Conference*, 2010, p. 177.
- <sup>22</sup>X. Cao, Y. Ye, and S. Liu, *Anal. Biochem.* **417**, 1 (2011).
- <sup>23</sup>M. J. Kwon, J. Lee, A. W. Wark, and H. J. Lee, *Anal. Chem.* **84**, 1702 (2012).
- <sup>24</sup>J. A. Capobianco, W. Y. Shih, Q. A. Yuan, G. P. Adams, and W. H. Shih, *Rev. Sci. Instrum.* **79**, 076101 (2008).
- <sup>25</sup>L. N. Loo, J. A. Capobianco, W. Wu, X. Gao, W. Y. Shih, W. H. Shih, K. Pourrezaei, M. K. Robinson, and G. P. Adams, *Anal. Chem.* **83**, 3392 (2011).
- <sup>26</sup>J. A. Capobianco, W. H. Shih, J. H. Leu, G. C. F. Lo, and W. Y. Shih, *Biosens. Bioelectron.* **26**, 964 (2010).
- <sup>27</sup>J. P. McGovern, W. Y. Shih, R. Rest, M. Purohit, Y. Pandya, and W. H. Shih, *Analyst* **133**, 649 (2008).
- <sup>28</sup>W. Wu, C. E. Kirimli, W.-H. Shih, and W. Y. Shih, *Biosens. Bioelectron.* **43**, 391 (2013).
- <sup>29</sup>W. Y. Shih, Q. Zhu, and S. Wei-Heng, *J. Appl. Phys.* **104**, 074503 (2008).
- <sup>30</sup>Q. Zhu, W. Y. Shih, and W.-H. Shih, *Appl. Phys. Lett.* **92**, 183505 (2008).
- <sup>31</sup>Q. Zhu, W. Y. Shih, and W.-H. Shih, *Sens. Actuators B* **138**, 1 (2009).
- <sup>32</sup>Q. Zhu, W.-H. Shih, and W. Y. Shih, *Sens. Actuators B* **182**, 147 (2013).
- <sup>33</sup>H. M. Duiker and P. D. Beale, *Phys. Rev. B* **41**, 490 (1990).
- <sup>34</sup>J.-K. Yang, W. S. Kim, and H.-H. Park, *Appl. Surf. Sci.* **169–170**, 544 (2001).
- <sup>35</sup>C. A. Randall, N. Kim, J. P. Kucera, W. W. Cao, and T. R. Shrout, *J. Am. Ceram. Soc.* **81**, 677 (1998).
- <sup>36</sup>M. Alguero, J. Ricote, R. Jimenez, P. Ramos, J. Carreaud, B. Dkhil, J. M. Kiat, J. Holc, and M. Kosec, *Appl. Phys. Lett.* **91**, 112905 (2007).
- <sup>37</sup>F. Griggio and S. Trolier-McKinstry, *J. Appl. Phys.* **107**, 024105 (2010).
- <sup>38</sup>R.-C. Chang, S.-Y. Chu, Y.-P. Wong, C.-S. Hong, and H.-H. Huang, *J. Alloys Compd.* **456**, 308 (2008).
- <sup>39</sup>R. A. Islam and S. Priya, *J. Mater. Sci.* **43**, 3560 (2008).
- <sup>40</sup>S. H. Hu, G. J. Hu, X. J. Meng, G. S. Wang, J. L. Sun, S. L. Guo, J. H. Chu, and N. Dai, *J. Cryst. Growth* **260**, 109 (2004).
- <sup>41</sup>P. Ferreira, R. Z. Hou, A. Y. Wu, M. G. Willinger, P. M. Vilarinho, J. Mosa, C. Laberty-Robert, C. Boissiere, D. Grosso, and C. Sanchez, *Langmuir* **28**, 2944 (2012).
- <sup>42</sup>H. Luo, W. Y. Shih, and W.-H. Shih, *J. Am. Ceram. Soc.* **90**, 3825 (2007).
- <sup>43</sup>M. C. Soylu, W.-H. Shih, and W. Y. Shih, *Ind. Eng. Chem. Res.* **52**, 2590 (2013).
- <sup>44</sup>ANSI/IEEE Std 176-1987, 1988, p. 0\_1.
- <sup>45</sup>E. P. Diamandis and T. K. Christopoulos, *Clin. Chem.* **37**, 625 (1991), available at <http://www.clinchem.org/content/37/5/625.full.pdf>.
- <sup>46</sup>Q. M. Zhang, H. Wang, N. Kim, and L. E. Cross, *J. Appl. Phys.* **75**, 454 (1994).
- <sup>47</sup>C.-Y. Hsieh, Y.-F. Chen, W. Y. Shih, Q. Zhu, and W.-H. Shih, *Appl. Phys. Lett.* **94**, 131101 (2009).
- <sup>48</sup>F. Xu, S. Trolier-McKinstry, W. Ren, B. Xu, Z.-L. Xie, and K. J. Hemker, *J. Appl. Phys.* **89**, 1336 (2001).